Role of Block Copolymer on the Coarsening of Morphology in Polymer Blend: Effect of Micelles

Chongwen Huang and Wei Yu
Dept. of Polymer Science and Engineering, Advanced Rheology Institute, Shanghai Jiao Tong University, Shanghai 200240, P.R. China

DOI 10.1002/aic.14633
Published online October 1, 2014 in Wiley Online Library (wileyonlinelibrary.com)

The reactive compatibilization of polystyrene/ethylene-α-octene copolymer (PS/POE) blend via Friedel–Crafts alkylation reaction was investigated by rheology and electron microscope. It was found that the graft copolymer formed from interfacial reaction reduced the domain size and decreased the coarsening rate of morphology. The reduction of the interfacial tension is very limited according to the mean field theory even assuming that all block copolymer stays on the interface. With the help of self-consistent field theory and rheological constitutive models, the distribution of graft copolymer was successfully estimated. It was found that large amount of copolymer had detached from the interfaces and formed micelles in the matrix. Both the block copolymer micelles in matrix and the block copolymers at the interface contribute to the suppression of coarsening in polymer blend, but play their roles at different stages of droplet coalescence. In droplet morphology, the micelles mainly hinder the approaching of droplets. © 2014 American Institute of Chemical Engineers *AIChE J*, 61: 285–295, 2015
Keywords: coarsening, polymer blend, morphology, rheology

Introduction

Polymer blends are widely used in various applications. Most commercially used polymers are immiscible, and need to be compatibilized during processing. Adding diblock copolymer with two segments miscible or partially miscible with two respective polymers is a convenient approach to compatibilize the blend, although nanoparticles with suitable surface treatment are also a choice.[1] A lot of efforts have been paid on how to choose the molecular structure,[2–6] molecular weight, concentration of copolymer,[7–9] and processing conditions.[10] In contrast to the fast transportation of surfactant in water/oil emulsion, the mobility of high molecular weight block copolymer is much lower and cannot necessarily move to the interface between two bulk polymers during finite mixing time. Moreover, the critical micelles concentration (CMC) of high molecular weight of copolymer is very low,[7–9,11] which makes it easier to form micelles and decreases the interfacial coverage. To solve the transportation problem of block copolymer from bulk to the interface, the so-called reactive blending technique that can produce block copolymer *in situ* during mixing is often adopted in industry.[12] Although the idea of reactive blending is to keep the block copolymer on the interface, high concentration of block copolymer can hardly stay at the interface especially under strong flow field.[13] Therefore, compatibilization mechanism of polymer blends with copolymer both on the interface and in the bulk polymer forming micelles is a general issue.

When the copolymer is on the interface, it has multiple influences on the interface dynamics.[14] It will decrease the interfacial tension between two polymers.[15] Its distribution at the interface is strongly flow dependent.[16,17] The nonhomogeneous distribution of copolymer at the interface will induce additional tangential stress, called Marangoni stress.[18] The effect of copolymer on the droplet deformation and breakup[19] is a result of competition between tip stretching and surface dilation, which depends mainly on the concentration of copolymer.[20] It is found that the critical capillary number decreases greatly in the presence of copolymer/surfactant,[21] which implies that smaller droplet can be obtained under the same mixing condition if copolymer/surfactant is added. The more important compatibilizing effect of copolymer is the retardance of coarsening both under shear flow and quiescent condition.[22–25] As interfacial tension controls the time scale of film drainage and droplet merge, its reduction also slows down the rate of coalescence according to several coalescence models.[26–30] The Marangoni stress has been suggested to retard the matrix film drainage and stabilize the morphology.[31,32] It is also suggested that the copolymer at the interface can act as a steric stabilizer to slow down droplet coalescence as compression of the surfactants in the matrix phase leads to an effective repulsion between approaching droplets.[33,34] Such mechanism can explain the coalescence suppression at low copolymer concentration where the interfacial tension is only slightly decreased.[22] All these effects require block copolymers to stay only at the interface, which is somewhat difficult especially when the

Additional Supporting Information may be found in the online version of this article.

Correspondence concerning this article should be addressed to W. Yu at wyu@sjtu.edu.cn.

block copolymer has a high molecular weight (and low critical micelle concentration) at high concentration and the blending is performed under strong flow field. As the quantitative analysis on the distribution of block copolymer is seldom performed, the above mechanisms on the morphology stabilization can only work at specified conditions without formation of micelles.

In this work, we will study the morphology stability in both physical and reactive blends of polystyrene (PS) and polyolefin elastomer (POE). The effect of graft copolymer on the coarsening behavior of reactive blends with droplet morphology and cocontinuous morphology will be illustrated. We will estimate the distribution of graft copolymer using rheology with the help of several constitutive models and self-consistent field theory for interfacial tension. We will suggest a new effect of micelles on the morphology stabilization during quiescent annealing in melt state.

Experimental

Materials

Polystyrene (PS, MC3700) with a density of 1.05 g/cm^3 was obtained from Chevron Philips Chemical. Ethylene-α-octene copolymer (POE, Engage 8150) was purchased from Dupont & Dow, with octene content of 25 wt % and a density of 0.868 g/cm^3 (20°C), and its molecular weight was determined to be 77 kg/mol (M_n) and 192 kg/mol (M_w).[35] Anhydrous $AlCl_3$ (analysis pure grade) was purchased from Shanghai Meixing Chemical Co. and used as received. Styrene, *n*-heptane, THF, methanol, and all other reagents were provided by Shanghai Reagent Co., China. All reagents were used without further purification.

Sample preparation and instrumental analysis

The melt blending process was carried out in a torque rheometer (XSS-300, Shanghai Kechuang Rubber & Plastic Equipment Co., China) at 180°C and 50 rpm for 10 min. For the reactive blending, $AlCl_3$ (0.3 wt % of the total polymer) was premixed with POE under the protection of a few drops of *n*-heptane and meantime styrene (1 wt % of the total polymer) was first added to the PS pellets, then POE and PS was added to the mixer simultaneously. All the blends were denoted as PS/POE *x*/*y*, where *x* and *y* represent the weight fraction of PS and POE in the blend, respectively. For comparison, neat PS and POE were also melt processed following the same procedure with or without the addition of catalyst and styrene. After melting blending, all the samples were compressed at 180°C under 10 MPa into disk-shape (of 25 mm diameter and 1 mm thickness) for rheological tests. To investigate the effect of annealing on the blend's morphology, specimens were annealed at a heating stage under 180°C for various times (15, 30, 60, 120, 180, and 240 min).

The viscoelastic behavior of the blends was measured by a stress controlled rotational rheometer (Bolin Gemini 200HR, Malvern Instrument, UK) with parallel-plate fixture (plate diameter of 25 mm and gap of 1 mm). Isothermal dynamic frequency sweep experiments were carried out at 180°C and the strain amplitude was chosen as 5% to ensure linear viscoelastic response. The frequency sweep was performed from 0.01 to 100 rad/s with five points per decade. There is no delay time and the integration is done for one oscillatory cycle. The total test time is about 1800 s and the first data point (0.01 rad/s) comes at about 630 s. As seen from SEM images of blends, the morphology is quite stable over this period for reactive blends, and only small increases in the droplet size and characteristic length of physical blends are expected. Thus, the influence of morphology change on the rheology data during measurement can be reasonably ignored.

To characterize the morphology of these blends, samples (unannealed and annealed blends) were first fractured in liquid nitrogen. Then, the morphology of fractured surface was measured via a field emission scanning electron microscopy (SEM, JSM-7401F, JEOL, Japan). To detect the distribution of reactive formed copolymer, reactive blended samples were cryogenically microtomed through a low temperature sectioning system (Ultracut UC6, Leica, Germany). Then, the microstructure was observed by a transmission electron microscopy (TEM, JEM-2100, JEOL, Japan) operating at an accelerating voltage of 200 kV. PS was selectively stained by RuO_4 to enhance the contrast.

The amount of copolymer formed during mixing was measured by Soxhlet extraction. Specifically, samples were first grounded into powders and then extracted in Soxhlet extractor by selective solvents, *n*-heptane for POE and THF for PS separately. First, the samples were extracted by the selective solvent of major component for 24 h, then another solvent was used to extract the minor component for another 24 h. This process was repeated twice, then the residue was vacuum dried and carefully weighed. The degree of graft was denoted as the mass ratio of residue (POE-*g*-PS) to the total.

The effect of catalyst on the degradation of PS was also evaluated. First, the PS component was extracted by THF, then the obtained PS/THF solution was filtered. Afterward, the filtrate was precipitated in excess of methanol, and then PS powder was collected and dried in vacuum oven. The molecular weight of PS was measured on gel permeation chromatography (Viscotek 270max triple-detector, Malvern Instruments, UK) with THF as eluent and a flow rate of 1.0 mL/min.

Results and Discussion

Coarsening of morphology

Although there are no reactive functional groups on both PS and POE chains, the benzene ring in PS can act as reactive site in the presence of Lewis acid, which is known as the Friedel–Crafts alkylation.[36] Aluminum chloride reacts with impurities like water to form a complex, which reacts further with unsaturated compounds (styrene in our work) forming the initial carbocation. The initial carbocation attacks POE, forming a macrocarbocation, which undergoes a chain scission through electron rearrangement. The fragments of POE chain can substitute for a proton from the benzene ring of PS, forming a POE-*g*-PS copolymer. The details of reaction mechanism are briefly summarized in Supporting Information. Scheme 1 illustrates the formation of graft copolymer POE-*g*-PS. Such reaction has been widely used to compatibilize polyolefin/PS blend[37–43] via reactive processing.

Typical SEM images of physical blends and reactive blends are shown in Figure 1. PS and POE are immiscible under the processing condition, and phase-separated morphology is seen in all blends. For PS/POE 20/80 physical blend, sea-island morphology is observed with the volume

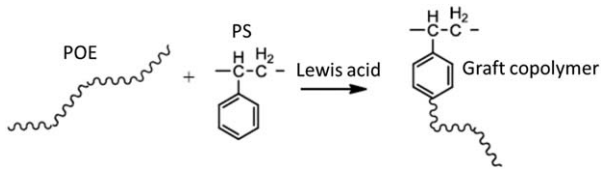

Scheme 1. Scheme of reaction between PS and POE in reactive blend.

average radius (R_v) about 0.37 μm. In PS/POE 20/80 reactive blend, the type of morphology does not change, but the droplet size decreases to about half of that in physical blends (0.20 μm). The interphases in reactive blend are also not as clear as those in physical blends. In 50/50 blend, cocontinuous morphology is observed in both physical blend and reactive blend. More significant decrease in characteristic length l_c[44] is seen in reactive blends. l_c of physical blend is about 4.82 μm, but becomes only 0.67 μm. The decrease in the size of phase domains is usually ascribed to the *in situ* formation of copolymers during reactive processing. The copolymers, when locates at the interface between two polymers, can lower the interfacial tension, which facilitates the breakup of domains into smaller ones due to the effective increase of actual capillary number.[22] Moreover, the copolymers at the interface can inhibit the coalescence of droplets through Marangoni stress[32,45] or steric hindrance.[33,34] The extent of decrease in domain size also depends on the composition of blends[43,46] due to the different efficiency of stress transfer from one phase to the other especially in viscoelastic asymmetric blend.

To illustrate the compatibilization effect of interfacial reaction, both physical blends and reactive blends were annealed under 180°C. SEM images of PS/POE 20/80 blends at different annealing time are shown in Figure 2. In contrast to the quick growth of droplet size in physical blends, the variation of droplet size in reactive blend is rather limited. Similar behavior is also observed in PS/POE 50/50 blend, where the coarsening of cocontinuous morphology in reactive blend is much slower than that in physical blend. Moreover, a great change in morphology of physical bends is also observed. As the annealing time increases, the cocontinuous morphology gradually breaks down and starts to change into a mixture with droplet morphology at about 60 min. It converts into completely droplet morphology at 240 min. In contrast, the cocontinuous morphology in 50/50 reactive blend is stable during long-time annealing. Such behaviors of coarsening have also been observed in different polymer blends,[8,47,48] especially although the copolymer will shrink the composition ranges of cocontinuous morphology after mixing, it can stabilize the cocontinuous morphology after annealing.[49]

Effect of interfacial tension and viscosity on coarsening

Quantitative variations in domain size from SEM images are shown in Figure 4. The droplet radius in PS/POE 20/80 blends increases linearly with time in both blends. The coarsening rate in physical blend is about 2.8×10^{-3} μm/min, which is significantly larger than that in reactive blend (about 0.56×10^{-3} μm/min). Theoretically, the coarsening of droplet morphology can be expressed as $R^n = R_0^n + k_i t$, where n is a mechanism dependent constant and k_i denotes the rate of coarsening. Classical theories such as the evaporation–condensation (or the so-called Ostwald ripening) mechanism[50,51] and the Brownian-coagulation mechanism[52,53] predict that the exponent n equals 3. In the coalescence mechanism suggested by Fortelný et al.,[54–56] n ranges from 3/2 to 5, depending on the mobility of interface and the driving force of coalescence such as gravity, Brownian motion, and van der Waals forces. The contact coalescence suggested by the present author predicts an almost constant coarsening rate ($n = 1$) at low volume fraction, low interfacial tension, and high matrix viscosity,[26,27] and the rate of coarsening is proportional to the interfacial tension and inversely proportional to the bulk viscosity. Such model implies that suppression of coarsening can happen either when the viscosity increases or the interfacial tension decreases.

In 50/50 physical blend, there is a quick linear growth of characteristic length within 30 min with the coarsening rate 0.18 μm/min. Then, the coarsening rate gradually slows down to about 0.01 μm/min after 120 min. The variation in coarsening rate is associated with the change of cocontinuous morphology into droplet morphology during annealing (Figure 3). Similar evolution of characteristic length is seen in 50/50 reactive blend, but the initial and final coarsening rate decreases substantially to 0.021 μm/min in 30 min and 0.83×10^{-3} μm/min after 120 min, respectively. Theoretical analysis on the coarsening of cocontinuous morphology is limited. Both the analysis based on the fiber stability[47,57] and Doi–Ohta model[8,58,59] have been adopted to describe the coarsening of cocontinuous morphology. In either case, the ratio between the interfacial tension and the viscosity determine the coarsening rate.

Both the contact coalescence model for droplet morphology and Doi–Ohta model for cocontinuous morphology imply that the coarsening of phase domain is proportional to the ratio between the interfacial tension and the effective viscosity of polymers. It is necessary to check the variation of these two quantities to understand the mechanism of coarsening. The reactive process during mixing involves the chain scission of polyolefin and addition of cocatalyst styrene monomer to PS, which may change the molecular weight of polymers and affect the shear viscosity. The dynamic moduli and complex viscosity of pure polymers and polymer/catalyst

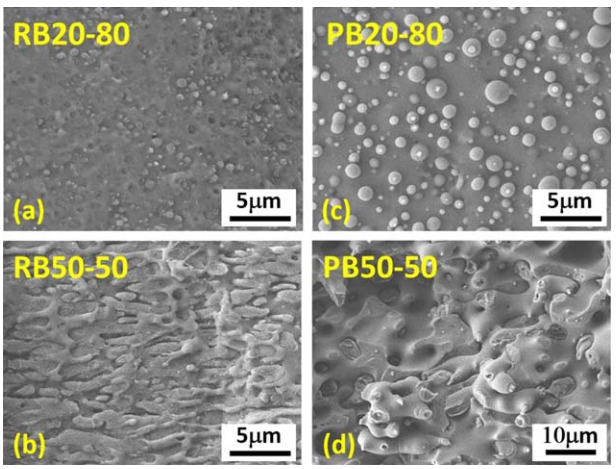

Figure 1. SEM images of PS/POE 20/80 (a), 50/50 (b) reactive blends, and 20/80 (c), 50/50 (d) physical blends.

[Color figure can be viewed in the online issue, which is available at wileyonlinelibrary.com.]

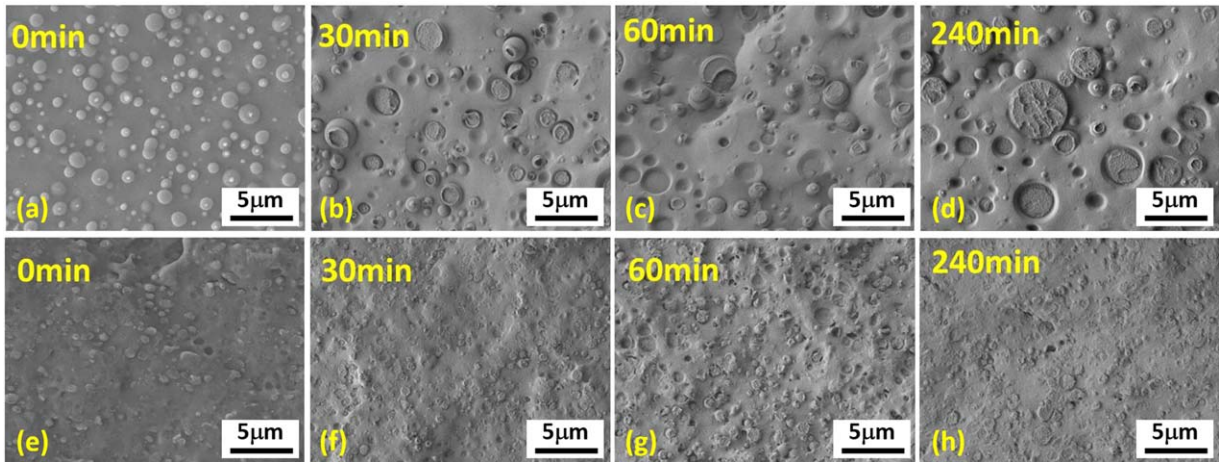

Figure 2. SEM images of PS/POE 20/80 physical blend (a–d) and reactive blend (e–h) annealed under 180°C for different times.

[Color figure can be viewed in the online issue, which is available at wileyonlinelibrary.com.]

are shown in Figure 5. For POE, both the dynamic moduli and complex viscosity decrease weakly after mixing with Lewis acid ($AlCl_3$), which manifests the degradation of POE during reactive processing. The decrease in the zero shear viscosity (η_0) of POE is only around 14%. For PS, the dynamic moduli and shear viscosity increase slightly at low frequency after mixing with the catalyst. This is ascribed to the addition of styrene monomer onto PS chain, which results in the simultaneous increase of weight average molecular weight (M_w) and number average molecular weight (M_n) (Table 1). The increase in η_0 of PS/catalyst as compared to pure PS is about 26%. However, the catalyst (Lewis acid) is not only distributed in PS in reactive blends. Only M_w increases slightly, but M_n is almost the same as the pure PS in reactive blends (Table 1). It means the variation of the effective viscosity in blend with droplet morphology and in blend with cocontinuous morphology is quite limited, which cannot explain the great reduction in the coarsening rate (5.1 times in 20/80 blend and 8.6–12 times in 50/50 blend) in reactive blends.

According to the theoretical models,[26,27,29] the other possible effect is the reduction of interfacial tension due to the distribution of copolymer at the interface. The amount of graft copolymer POE-*g*-PS is determined by a two-step Soxhlet extraction using solvents of POE and PS, respectively. The weight fraction of graft copolymer is 10% in PS/POE 20/80 reactive blend and is 18% in PS/POE 50/50 reactive blend. If all the copolymers are assumed to stay on the interface, the interfacial coverage of copolymer can be estimated as[34]

$$\Sigma = \frac{N_{av}\rho_{copolymer}\phi_{copolymer}/M_{copolymer}}{S_{sp}} \quad (1)$$

N_{av} is Avogadro constant. $M_{copolymer}$ is the molecular weight of copolymer (145 kg/mol), which is the sum of M_n for PS chain (111 kg/mol) and POE segment (34 kg/mol). According to the reaction mechanism, chain scission of POE takes place before the POE segment is grafted onto the PS chain. Then, the molecular weight of POE segment is assumed to be half of the whole chain. $\rho_{copolymer}$ is the density of copolymer (0.99 g/cm^3), which is estimated from the weight fraction of PS and POE in graft copolymer. $\phi_{copolymer}$ is the volume fraction of graft copolymer. S_{sp} is the specific interfacial area per unit volume, $S_{sp}=3\phi/R$ for droplet morphology and $S_{sp}=3\pi a(1-a)/2l_c$ for cocontinuous morphology,[44] where ϕ is the volume fraction of droplet phase and

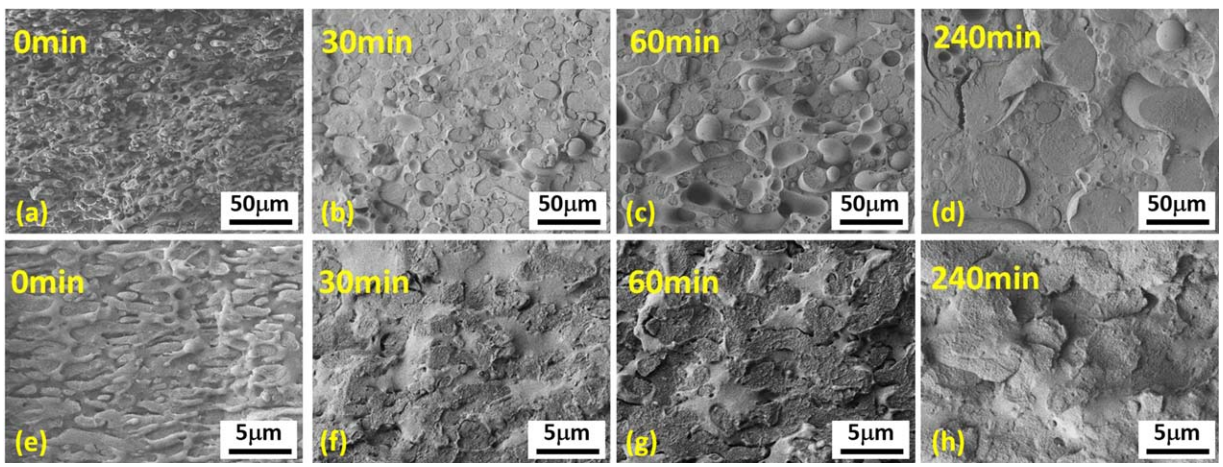

Figure 3. SEM images of PS/POE 50/50 physical blend (a–d) and reactive blend (e–h) annealed under 180°C for different times.

[Color figure can be viewed in the online issue, which is available at wileyonlinelibrary.com.]

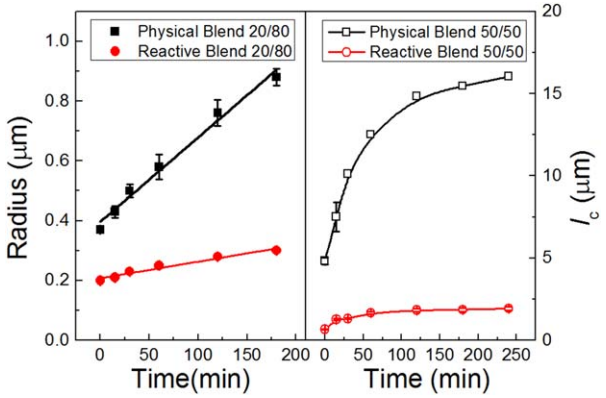

Figure 4. Evolution of mean radius with annealing time in PS/POE 20/80 blends and characteristic length in PS/POE 50/50 blends.

[Color figure can be viewed in the online issue, which is available at wileyonlinelibrary.com.]

$\phi=3a^2-2a^3$ in cocontinuous blend. The interfacial coverage of copolymer is about 0.13 chain/nm^2 in PS/POE 20/80 reactive blend and 0.41 chain/nm^2 in 50/50 reactive blend. The effect of graft copolymer on the interfacial tension can be estimated using the mean field theory[60–63]

$$\frac{\Gamma}{\Gamma_0}=1-\frac{1}{\sqrt{\chi N}}f\left(z/R_g\right) \tag{2}$$

where $z/R_g=\sqrt{6N}V_{0,\mathrm{ref}}\Sigma/bN_{\mathrm{av}}$ and $f(x)=1.38x-0.52x^2+0.45x^3$. $V_{0,\mathrm{ref}}$ is the reference volume (12.25cm^3/g),[40] and N is the polymerization of copolymer, b is the Kuhn length. χ is the Flory–Huggins interaction parameter, which is 0.0629 at 180°C if the interaction between PS and polyethylene is adopted.[64] Γ and Γ_0 are the interfacial tension of compatibilized and clean interface, respectively. The interfacial tension Γ is estimated to be $0.97\Gamma_0$ for PS/POE 20/80 reactive blend and $0.90\Gamma_0$ for PS/POE 50/50 reactive blend. The decrement of interfacial tension is rather small, which is mainly attributed to the much larger molecular weight of copolymer in this work as compared to those in literatures.[60–63] It means that even all the generated copolymers are located at the interface, the reduction in interfacial tension is very limited in 20/80 blend. Such small decrease in interfacial tension cannot explain the great slowdown of coarsening rate in reactive blends.

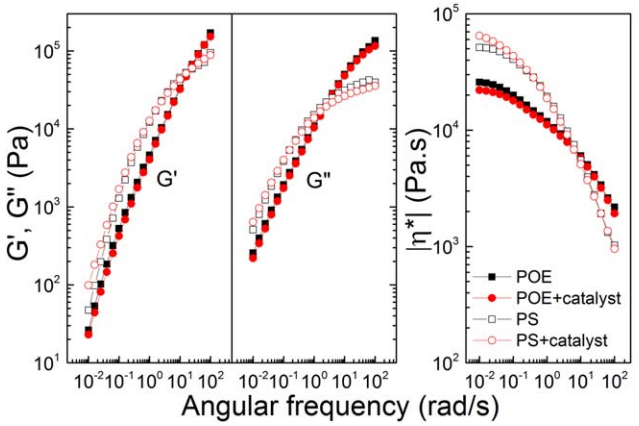

Figure 5. Effect of catalyst on the dynamic moduli and complex viscosity of PS and POE at 180°C.

[Color figure can be viewed in the online issue, which is available at wileyonlinelibrary.com.]

Role of interfacial copolymer and micelles

Other mechanisms for the compatibilization effect concern about the role of copolymer during coalescence. In the droplet coalescence model, droplets first approach each other either under shear flow or under quiescent condition. Parallel film is formed between two droplets, followed by the drainage of the matrix fluid trapped between droplets until the critical film thickness is reached, where the film is highly unstable due to the van der Waals interactions. Then, the matrix film is ruptured and two droplets merge into one droplet. Drainage of matrix out of the film and the thinning of film is the key step in droplet coalescence. During the drainage of matrix fluid, the copolymer will also be expelled from the film and cause the nonuniform distribution of copolymer. Someone argues that the Marangoni stress due to the nonhomogeneous distribution of copolymer at the interface will act as a driving force for the rehomogeneity of copolymer, which prevents the coalescence of two droplets.[32]

Others argue that the entropic repulsion of copolymer chains at the surface will balance van der Waals attractions, and the coalescence of droplets is inhibited due to the steric hindrance of copolymer.[34] The latter effect strongly relies on interfacial coverage, chain length, and the status of "brush" at the interface.[65] The saturated coverage of copolymer can be calculated from Eq. 2 as $\Sigma_0=1.3\mathrm{chain/nm}^2$ when the interfacial tension becomes zero. Then, the percent of interfacial coverage (Σ/Σ_0) is 9.5% and 31.1% for 20/80 and 50/50 reactive blends, respectively. The critical interfacial concentration Σ_c to prevent coalescence depends on the average of the squares of the relaxed chain end-to-end distance copolymer, and Σ_c/Σ_0 has been estimated to be as low as 1%.[34] Because the copolymer can move out of the contact area, the actual value of Σ_c is expected to be much higher. The typical range of critical coverage Σ_c/Σ_0 is round 10–20%,[34] which depends on the molecular weight of copolymers. As the above estimated interfacial coverage falls into this range, it seems that the slowdown of coarsening in this work can be explained by the steric hindrance of copolymer.

However, such value of interfacial coverage is based on the assumption that all copolymers stay at the interface, which is probably not the fact. Actually, when we look into more details about the morphology, it is readily to see large amount of tiny droplets in tens of nanometer near large PS domains in both PS/POE 20/80 reactive blend and 50/50 reactive blend (Figures 6a–d), while these tiny droplets are almost absent in physical blends (Figures 6e, f). For reactive blends, two groups of droplets (large one and small one) can be seen for both 20/80 blend and 50/50 blend, where the large droplets have a radius about 0.4 μm in 20/80 blend and the radius of small droplets is 20–30 nm in both blends. In fact, the estimation on the interfacial coverage of copolymer is based on the interfacial area using the droplet radius (or characteristic length) from SEM images, that is, only the large droplets are counted. If the interface of small droplets is also included, the mean interfacial coverage of copolymer would become lower than the above values. Moreover, it is believed that the copolymers are not uniformly distributed on the interface of large droplet and small droplets. Copolymer concentration on small droplets interface is much higher than

Table 1. The Molecular Weights of Polystyrene in Different Blends

Samples	PS	PS/Catalyst	PS/POE 20/80 (Physical Blend)	PS/POE 20/80 (Reactive Blend)	PS/POE 50/50 (Physical Blend)	PS/POE 50/50 (Reactive Blend)
M_n (kg/mol)	118	138	114	115	112	107
M_w (kg/mol)	264	315	253	338	272	328
M_w/Mn	2.22	2.28	2.22	2.93	2.43	3.06

that on large droplets interface because the small droplets are regarded as the micelles (or "swollen" micelles) formed by POE-*g*-PS copolymer during mixing. Such phenomenon has been observed in many polymer blends which are compatibilized either by premade copolymer or by copolymer from *in situ* interfacial reaction.[7,34,66,67] Although it is difficult to estimate the amount of copolymers that are detached from the interface to form micelles just from the TEM images, it is believed that the interfacial coverage of copolymer on interfaces between PS and POE can be greatly reduced.

One may argue if these small droplets are crosslinked gel particles. It is believed that the probability of crosslinking is quite low in our system. First, there is no space filling gel in reactive blends as shown from linear viscoelasticity using Winter–Chambon criteria.[68] This is consistent with the findings of Guo et al.,[41] who adopted the amount of $AlCl_3$ 1.2 wt %, much higher than that (0.3 wt %) in our work. Second, chain scission/coupling in neat polymer can happen in the presence of catalyst. This can be seen from the change in molecular weight of PS in reactive blends (Table 1). Although the molecular weight of POE in reactive blends is not measured, chain scission/coupling reactions are also expected in POE domains. Because these reactions happen in the presence of catalyst, it is highly possible that the catalyst locates both in the bulk and interfacial area in reactive blends. However, even all catalysts are located in one component (PS or POE), it cannot result in crosslinking of PS or POE. This is clearly illustrated in Figure 5. Thus, the crosslinking in either domain is not possible. Third, as both PS and POE can be regarded as multifunctional, it is possible that multiple reactions happen between PS molecules and POE molecules, which may result in highly branched (or crosslinked) copolymer with high molecular weight. In fact, interfacial crosslinking in reactive blending with multifunctional components have been reported in literatures.[69,70] Our previous works[46,71] have shown that the efficiency of catalyst and the amount of catalyst are two main factors to influence the multiple reactions between two molecules in the interfacial area. In our reactive system, the low amount of catalyst in the interfacial area decreases the possibility of interfacial crosslinking.

Actually, the distribution of copolymer can also be evaluated by rheology. The storage modulus of physical blends is shown in Figure 7. For PS/POE 20/80 blend, Palierne model[72] is used to fit the storage modulus of blend due to the droplet morphology. The best fit gives the interfacial tension about 1.0 mN/m using $R_v = 0.37$ μm as obtained from SEM analysis. For PS/POE 50/50 blend with cocontinuous morphology, the storage modulus of blend is fitted by YZZ model[44] using $l_c = 4.82$ μm. Again, the interfacial tension of 1.0 mN/m is obtained. Such value of interfacial tension between PS and POE is well consistent with the extrapolated value (1.6 mN/m) from those determined between 200°C and 220°C using short fiber retraction method.[73] Complete comparisons on dynamic moduli and complex viscosity between experiments and model fittings for physical blends are shown in Supporting Information Figure S1. The fittings are generally good for both G′ and complex viscosity in both blends. In reactive blends, as shown in Figure 8, if the same model with the same interfacial tension is adopted, the model predictions agree with the experimental data only at high frequency and is evident smaller than the experimental

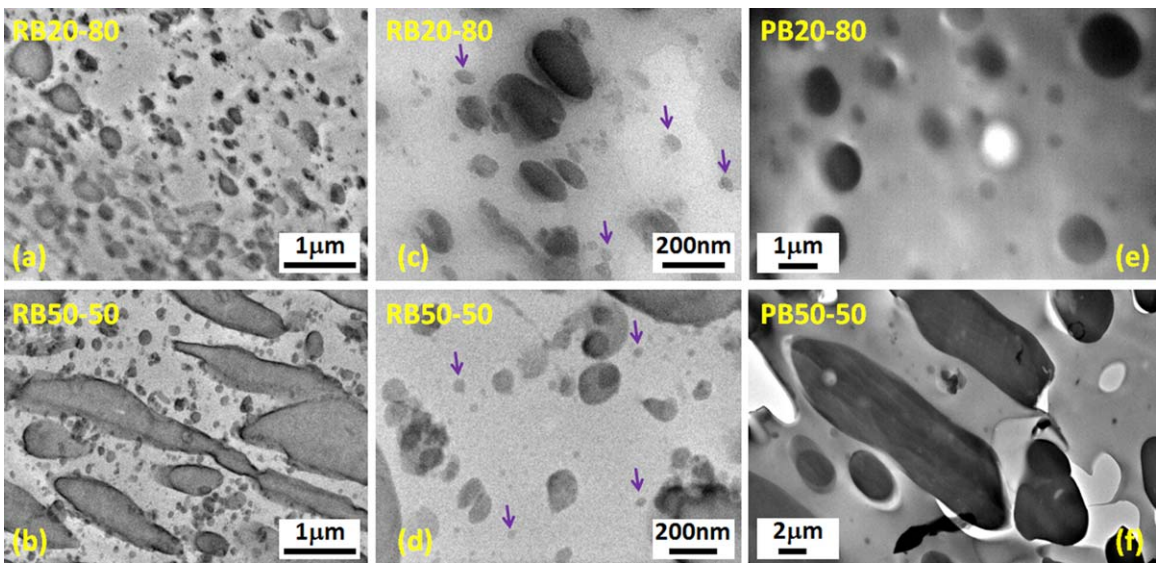

Figure 6. TEM images of PS/POE 20/80 reactive blend (a, c) and 50/50 reactive blend (b, d). (c) and (d) are amplification of (a) and (b), respectively. (e) and (f) are TEM images of PS/POE 20/80 and 50/50 physical blends, respectively.

[Color figure can be viewed in the online issue, which is available at wileyonlinelibrary.com.]

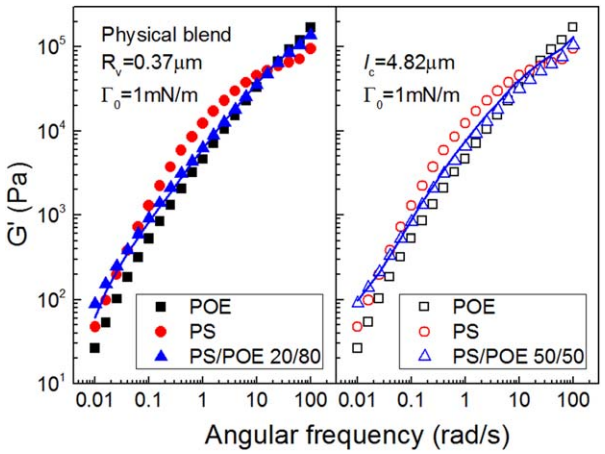

Figure 7. Storage moduli of PS/POE 20/80 physical blend (left) and 50/50 physical blend (right) at 180°C.

The solid line in the left panel denotes the fit of Palierne model with $R_v = 0.37$ μm and $\Gamma_0 = 1$ mN/m. The solid line in the right panel denotes the fit of YZZ model with $l_c = 4.82$ μm and $\Gamma_0 = 1$ mN/m. [Color figure can be viewed in the online issue, which is available at wileyonlinelibrary.com.]

data at low frequencies. Such phenomenon is seen in 20/80 blend with droplet morphology as well as in 50/50 blend with cocontinuous morphology. If the interfacial tension calculated by self-consistent mean-field theory (SCMFT) is adopted, the storage modulus will become even smaller at low frequency due to the slight decrease in the interfacial tension in the presence of copolymer. It has been reported that additional relaxation process can be observed in compatibilized blend with droplet morphology, which can also be described by Palierne model with anisotropic interfacial tension.[74–77] However, the deviation of the isotropic Palierne model (short dash line in the left panel of Figure 8) from the experimental data is too large, and cannot be compensated by only introducing an interfacial elastic modulus (see Supporting Information for details). Moreover, there is no theoretical model for the viscoelastic interface in cocontinuous morphology.

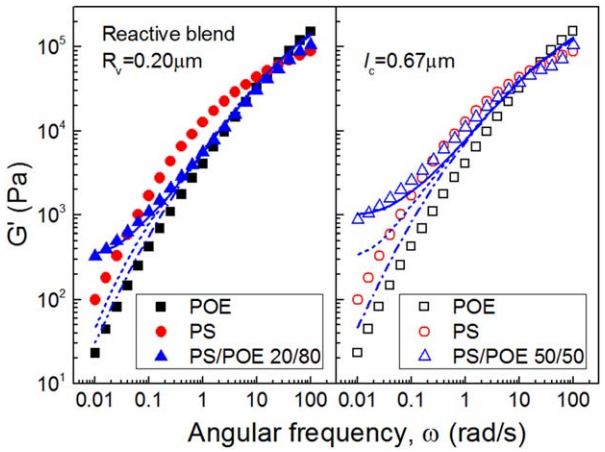

Figure 8. Storage moduli of PS/POE 20/80 reactive blend (left) and 50/50 reactive blend (right) at 180°C.

The short dash line in the left panel denotes the prediction of Palierne model with $R_v = 0.20$ μm and $\Gamma = \Gamma_0 = 1$ mN/m. The short dash line in the right panel denotes the prediction of YZZ model with $l_c = 0.67$ μm and $\Gamma = \Gamma_0 = 1$ mN/m. The dash-dot lines represent the predictions of corresponding models with zero interfacial tension. The solid lines represent the model predictions with additional contributions from micelles. The micelles are assumed to be "unswollen" and $\Gamma_m = 0.2\Gamma_0 = 0.2$ mN/m. [Color figure can be viewed in the online issue, which is available at wileyonlinelibrary.com.]

In contrast to two-phase model which considers the contribution from PS domain and POE domain with isotropic (or anisotropic) interface, a third copolymer rich phase (micelles) will have additional contribution to the dynamic modulus. In such three-phase model, the contributions from PS domain and POE domain can be calculated by Palierne model or YZZ model, depending on the morphology. The contribution from micelles is similar to that of droplet phase,[78,79] but with a completely different interfacial viscoelasticity. Therefore, the storage modulus of reactive blend $G'_{rb}(\omega)$ can be expressed as

$$G'_{rb}(\omega) = G'_{b}(\omega) + G'_{sm}(\omega) \tag{3}$$

where $G'_{b}(\omega)$ is the predictions using Palierne model (20/80 blend) and YZZ model (50/50 blend). The contribution from micelles can be calculated by a model recently suggested by Yu and Zhou,[80] which considers the effects of interfacial slip, interfacial thickness, and interfacial viscosity on the droplet deformation and rheology of emulsion

$$G'_{sm}(\omega) = \frac{2Kf_2^2\omega^2\tau^2}{3\left(\omega^2\tau^2 + f_1^2\right)} \tag{4}$$

where

$$K = \frac{6\Gamma_m}{5R}\frac{(\lambda+1)(2\lambda+3)\varphi}{5(\lambda+1)-(5\lambda+2)\varphi}, \tau = \eta_m R/\Gamma_m \tag{5}$$

with R the droplet radius, λ the ratio between the droplet viscosity (η_d) and matrix viscosity (η_m), and φ the volume fraction of micelle droplet. Γ_m is the interfacial tension of micelles in POE. f_1 and f_2 depends only on viscosity ratio for viscous blend with simple interface, that is, the interface is isotropic and interfacial tension is the only variable to quantify the interfacial property.[79,81] For viscous interface, it is suggested[80]

$$f_1 = \frac{8}{g}(5+5\lambda+2(2+3q)\Lambda+25C_n\lambda/\Lambda) \tag{6}$$

$$f_2 = \frac{5}{g}(16+19\lambda+8(1+3q)\Lambda+80C_n\lambda/\Lambda) \tag{7}$$

$$g = 38\lambda^2+\lambda(89+(52+46q)\Lambda)+16\left(3+(3+4q)\Lambda+2q\Lambda^2\right) +2(120+95\lambda+4(9+q)\Lambda)C_n\lambda/\Lambda \tag{8}$$

where the ratio between the interfacial capillary number and the capillary number is known as the Boussinesq number, $\Lambda = Ca_s/Ca = \mu/\eta_m R$, with μ the interfacial shear viscosity. $q = \kappa/\mu$ is the ratio between the interfacial dilatational viscosity (κ) and the interfacial shear viscosity (μ). $C_n = a_I/R$ is the Cahn number, defined as the ratio between the interfacial thickness (a_I) and the radius of droplet.

Yu–Zhou model (Eqs. 3–8) is continuum model, which considers the finite interfacial thickness and interfacial

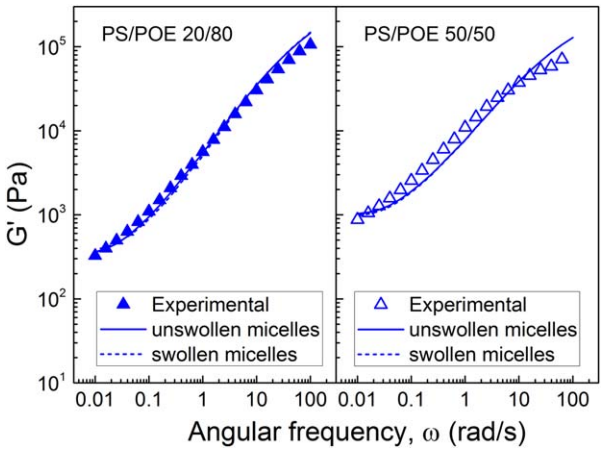

Figure 9. Comparison of model prediction with the experimental storage modulus of 20/80 blend and 50/50 blend.

Solid lines correspond to the "unswollen" micelles, while short dash lines correspond to the "swollen" micelles. [Color figure can be viewed in the online issue, which is available at wileyonlinelibrary.com.]

viscoelasticity. It is necessary to define the Boussinesq number, the Cahn number, and the interfacial viscosity ratio when it is adopted to describe the behavior of micelles. In the entangled case, the Boussinesq number can be approximated as $\Lambda = \frac{1}{2}(a_I/R_g)^2$,[80,82] where R_g is the radius of gyration of copolymer ($\approx b/\sqrt{6/N} \approx 23.4$ nm). In the micelles of POE-*g*-PS, it is reasonable to assume that the interfacial thickness is around the half of the radius of unswollen micelles if the wettability of copolymer inside and outside the droplet is similar. The typical radius of micelles is 20–30 nm, which gives the Boussinesq number about 0.09–0.2 and the Cahn number about 0.5. It is hard to estimate the interfacial viscosity ratio q, however, its effect is limited. The variation of G'_{sm} at 0.01 rad/s is within 5% when q ranges from 0 to 100.

For unswollen micelles, it is assumed that the droplet size is smaller and the radius 20 nm is adopted. The corresponding Boussinesq number is 0.09. The volume fraction of micelles particles is calculated from its weight fraction to be 9.2% in 20/80 blend and 17.5% in 50/50 blend. It is assumed here that all copolymers are detached from the PS droplets and form micelles. This is a limiting situation, which helps to estimate the maximum contribution to rheology from micelles. In such limiting case that all copolymers forms "unswollen" micelles, the volume fraction of PS becomes 11.9% in PS/POE 20/80 reactive blend and 35.4% in PS/POE 50/50 reactive blend. Model predictions with the contributions from micelles are shown as solid lines in Figure 8. According to the self-consistent field theory,[15,83] copolymers with concentrations higher than CMC tend to form highly swollen micelles, and the interfacial tension depends on the asymmetry of copolymer.[84] The interfacial tension between micelles and POE is fitted to be 0.2 mN/m, which is 20% of clean interface. Detailed comparisons on dynamic moduli and complex viscosity are given in Supporting Information Figure S2. For PS/POE 20/80 blend, with the additional contribution from micelles using Yu–Zhou model, theories can give quite good prediction on both G′ and complex viscosity, especially at low frequency. The deviation at high frequency is attributed to the inaccuracy of the components' dynamic moduli. The rheology data of PS/catalyst and POE/catalyst (Figure 5) are used in modeling reactive blends to account for possible reactions of components. The difference in the reactions of components in pure polymer and in blends causes such deviation. For PS/POE 50/50 reactive blend, although the deviation at high frequency still exists, the fitting at low frequency regime is acceptable but is not so good as that in 20/80 blend due to more complex morphology in 50/50 blend.

Because of the size distribution of the nanoscale droplets, it is highly possible that the small droplets are not pure micelles. Some "swollen" micelles should exist. The other limiting case is considered here, that is, all the small droplets are swollen micelles. For swollen micelles, it is assumed that the droplet size is larger and the radius 30 nm is adopted. The corresponding Boussinesq number is 0.2. In the fitting, it is assumed that 5% of PS is adsorbed in the micelles. Then, the volume fraction of micelles droplets becomes 14.2% in 20/80 blend and 22.5% in 50/50 blend. The volume fraction of PS domains decreases correspondingly. A comparison between the prediction of "unswollen" and "swollen" micelles is shown in Figure 9. Detailed comparisons on dynamic moduli and complex viscosity for swollen micelles are given in Supporting Information Figure S3. The prediction of swollen case is slightly smaller than that of unswollen case, and both results are quite close to experimental data as compared with the predictions of two-phase models. Simple micelles and swollen micelles are two limiting situations. In fact, the size distribution of micelles corresponds to different extent of swelling. The very close model predictions for these two limiting cases imply that the picture of micelles are consistent with the rheology data even when the polydispersity of micelles are considered, although it might be difficult to determine the extent of swelling quantitatively.

Although the exact amount of copolymer that locates at PS/POE interface and that forms micelles are hard to determine, the success of three-phase model suggests that a large amount of copolymer forms micelles. Therefore, both rheology and TEM implies that the actual interfacial coverage of copolymer on large droplets (micron-scale) can be much lower than the critical coverage, and it becomes doubtable whether the steric hindrance of copolymer is the only reason to prevent droplet coalescence (Figure 10a). During the coarsening of morphology, coalescence between small droplets (micelles), between micelles and micron-scale droplets, and between micron-scale droplets will cause the increase of average droplet size. The coalescence involving nanoscale droplets is actually difficult due to the steric effect of copolymers on the interface of nanoscale particles, that is, micelles and swollen micelles. The coalescence between micron-scale droplets is also difficult although the copolymer content on its interface is expected to be low. Consider the quiescent coalescence process of droplet morphology, the key step is the formation and drainage of matrix film between two adjacent droplets which are in contact initially or after certain time of thermal motion. In the blends without micelles (or "swollen" micelles), droplet can readily get into touch with each other and the drainage process can be hindered by the presence of copolymer on the interface. In contrast, the existence of micelles can act as obstacles to prevent large droplets approaching each other. In another words, the contact probability instead of the drainage

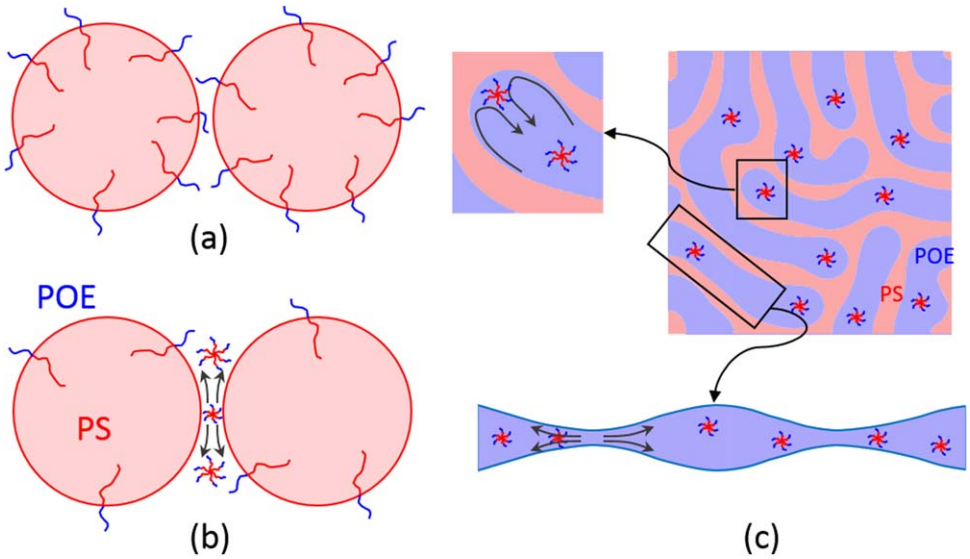

Figure 10. Coarsening mechanism of polymer blends with copolymer located at the interfaces (a) and forming large amount of copolymer micelles (b, c).

The arrows indicate the directions of flow, which is generated by different processes such as droplet approaching (b), capillary instability and curvature driven flow (c). [Color figure can be viewed in the online issue, which is available at wileyonlinelibrary.com.]

probability is reduced greatly due to the presence of micelles. The stability of micelles during quiescent annealing becomes important. In our case, large molecular weight of copolymer generates $\chi N_{copolymer}=128$, which is large enough ($>>20$) that spontaneous micelle dissolution and reformation can be negligible at the equilibrium critical micelle concentration.[9] Actually, in theories concerning the coarsening of droplets,[26,27,85] the contact probability is a statistical value depending only on the volume fraction and the droplet size,[86–88] where the process of getting touched is regarded to be faster than the drainage and merging process. The formation of micelles does not change the nearest-neighbor distribution of droplets, but slows down the translational motion of droplets by decrease the apparent diffusion coefficient. Such mechanism is schematically represented in Figure 10b. For cocontinuous morphology, it has been suggested that thread stability[48,89,90] and curvature driven flow[30,53,91] are possible mechanisms for the coarsening. In the thread stability analysis, the rate of coarsening is correlated with the rate of growth of the dominant disturbance. The existence of copolymer micelles also prevent the development of the dominant disturbance (Figure 10c), although such mechanism is unlikely dominating as the requirement for large aspect ratio of thread (>10) is hardly satisfied in cocontinuous morphology of polymer blends. In the curvature driven flow mechanism, the coarsening of cocontinuous morphology is caused by the capillary flow within the interconnected channels, while the presence of copolymer micelles can also be obstacles to hinder the flow. As compared to copolymer molecules, the copolymer micelles are much larger in size and more effective in slowing down or even preventing the flow during coarsening of large droplets.

Conclusions

In this work, we studied the reactive blending of immiscible polymers, PS and POE, in the presence of Lewis acid. It is found that not only the domain size is greatly reduced by introducing interfacial reaction, but the stability of morphology during annealing in melt state is significantly enhanced, that is, the coarsening rate of morphology in reactive blends becomes much lower than that in physical blends. The change in bulk viscosity during reactive mixing and the decrease in the interfacial tension are proved to have minor effect on the coarsening kinetics. Both TEM observation and rheology analysis support the statement that many copolymers have detached from the interface and form micelles (or swollen micelles) in polymer matrix. Therefore, the mechanism of morphology stabilization can be ascribed to the steric effect of block copolymers at interface as well as micelles, but they play the roles at different stages of droplet coalescence. In droplet morphology, the micelles slow down the approaching velocity while the steric effect of block copolymer at interface extend the drainage time. Both effects will suppress coarsening in polymer blends.

Acknowledgments

The authors thank the support from the National Basic Research Program of China (973 Program) 2012CB025901 and the National Natural Science Foundation of China (No. 21074072). W. Yu is supported by the Program for New Century Excellent Talents in University and the SMC project of Shanghai Jiao Tong University.

Literature Cited

1. Li Q, Huang YJ, Xi S, Yang Q, Li GX. Double emulsions of immiscible polymer blends stabilized by interfacially active nanoparticles. *AIChE J*. 2013;59:4373–4382.
2. Kim J, Gray MK, Zhou H, Nguyen ST, Torkelson JM. Polymer blend compatibilization by gradient copolymer addition during melt processing: stabilization of dispersed phase to static coarsening. *Macromolecules*. 2005;38:1037–1040.
3. Zhang CL, Feng LF, Zhao J, Huang H, Hoppe S, Hu GH. Efficiency of graft copolymers at stabilizing co-continuous polymer blends during quiescent annealing. *Polymer*. 2008;49:3462–3469.
4. Pu GW, Luo YW, Lou Q, Li BG. Co-continuous polymeric nanostructures via simple melt mixing of PS/PMMA. *Macromol Rapid Commun*. 2009;30:133–137.

5. Zhang CL, Feng LF, Gu XP, Hoppe S, Hu GH. Blend composition dependence of the compatibilizing efficiency of graft copolymers for immiscible polymer blends. *Polym Eng Sci*. 2010;50:2243–2251.
6. Lepers JC, Favis BD. Interfacial tension reduction and coalescence suppression in compatibilized polymer blends. *AIChE J*. 1999;45:887–895.
7. Lyu S, Jones TD, Bates FS, Macosko CW. Role of block copolymers on suppression of droplet coalescence. *Macromolecules*. 2002; 35:7845–7855.
8. Galloway JA, Jeon HK, Bell JR, Macosko CW. Block copolymer compatibilization of cocontinuous polymer blends. *Polymer*. 2005; 46:183–191.
9. Bell JR, Chang K, López-Barrón CR, Macosko CW, Morse DC. Annealing of cocontinuous polymer blends: effect of block copolymer molecular weight and architecture. *Macromolecules*. 2010;43: 5024–5032.
10. Zhang CL, Feng LF, Hoppe S, Hu GH. Compatibilizer-tracer: a powerful concept for polymer-blending processes. *AIChE J*. 2012;58: 1921–1928.
11. Marić M, Macosko CW. Block copolymer compatibilizers for polystyrene/poly(dimethylsiloxane) blends. *J Polym Sci Part B: Polym Phys*. 2002;40:346–357.
12. Baker W, Scott C, Hu GH. Reactive Polymer Blending. Munich: Hanser, 2001.
13. Charoensirisomboon P, Chiba T, Solomko SI, Inoue T, Weber M. Reactive blending of polysulfone with polyamide: a difference in interfacial behavior between in situ formed block and graft copolymers. *Polymer*. 1999;40:6803–6810.
14. Van Puyvelde P, Velankar S, Moldenaers P. Rheology and morphology of compatibilized polymer blends. *Curr Opin Colloid Interface Sci*. 2001;6:457–463.
15. Chang K, Macosko CW, Morse DC. Ultralow interfacial tensions of polymer/polymer interfaces with diblock copolymer surfactants. *Macromolecules*. 2007;40:3819–3830.
16. Jeon HK, Macosko CW. Visualization of block copolymer distribution on a sheared drop. *Polymer*. 2003;44:5381–5386.
17. Narayanan B, Ganesan V. Flow deformation of polymer blend droplets and the role of block copolymer compatibilizers. *Phys Fluids*. 2006;18:042109.
18. Stone HA. Dynamics of drop deformation and breakup in viscous fluids. *Annu Rev Fluid Mech*. 1994;26:65–102.
19. Stone HA, Leal LG. The effects of surfactants on drop deformation and breakup. *J Fluid Mech*. 1990;220:161–186.
20. Eggleton CD, Pawar YP, Stebe KJ. Insoluble surfactants on a drop in an extensional flow: a generalization of the stagnated surface limit to deforming interfaces. *J Fluid Mech*. 1999;385:79–99.
21. de Bruijn RA. Deformation and breakup of drops in simple shear flows. Ph.D. thesis. Tech. Univ. Eindhoven, Eindhoven, 1991.
22. Hu YT, Pine DJ, Leal LG. Drop deformation, breakup, and coalescence with compatibilizer. *Phys Fluids*. 2000;12:484–489.
23. Lyu SP, Bates FS, Macosko CW. Coalescence in polymer blends during shearing. *AIChE J*. 2000;46:229–238.
24. Perilla JE, Jana SC. Coalescence of immiscible polymer blends in chaotic mixers. *AIChE J*. 2005;51:2675–2685.
25. Martin JD, Velankar SS. Effects of compatibilizer on immiscible polymer blends near phase inversion. *J Rheol*. 2007;51:669–692.
26. Yu W, Zhou CX, Inoue T. A coalescence mechanism for the coarsening behavior of polymer blends during a quiescent annealing process. I. Monodispersed particle system. *J Polym Sci Part B: Polym Phys*. 2000;38:2378–2389.
27. Yu W, Zhou CX, Inoue T. A coalescence mechanism for the coarsening behavior of polymer blends during a quiescent annealing process. II. Polydispersed particle system. *J Polym Sci Part B: Polym Phys*. 2000;38:2390–2399.
28. Lyu SP, Bates FS, Macosko CW. Modeling of coalescence in polymer blends. *AIChE J*. 2002;48:7–14.
29. Doi M, Ohta T. Dynamics and rheology of complex interfaces. *I. J Chem Phys*. 1991;95:1242–1248.
30. López-Barrón CR, Macosko CW. A new model for the coarsening of cocontinuous morphologies. *Soft Matter*. 2010;6:2637–2647.
31. Chesters AK, Bazhlekov IB. Effect of insoluble surfactants on drainage and rupture of a film between drops interacting under a constant force. *J Colloid Interface Sci*. 2000;230:229–243.
32. Milner ST, Xi H. How copolymers promote mixing of immiscible homopolymers. *J Rheol*. 1996;40:663–687.
33. Sundararaj U, Macosko CW. Drop breakup and coalescence in polymer blends: the effects of concentration and compatibilization. *Macromolecules*. 1995;28:2647–2657.
34. Macosko CW, Guégan P, Khandpur AK, Nakayama A, Marechal P, Inoue T. Compatibilizers for melt blending: premade block copolymers. *Macromolecules*. 1996;29:5590–5598.
35. Liu JY, Yu W, Zhou CX. The effect of shear flow on reaction of melt poly(ethylene-a-octene) elastomer with dicumyl peroxide. *Polymer*. 2006;47:7051–7059.
36. Morrison RT, Boyd RN. *Organic Chemistry*, 3rd ed. New York: Allyn and Bacon, 1976.
37. Sun YJ, Baker WE. Polyolefin/polystyrene in situ compatibilization using Friedel–Crafts alkylation. *J Appl Polym Sci*. 1997;65:1385–1393.
38. Sun YJ, Willemse RJG, Liu TM, Baker WE. In situ compatibilization of polyolefin and polystyrene using Friedel-Crafts alkylation through reactive extrusion. *Polymer*. 1998;39:2201–2208.
39. Diaz MF, Barbosa SE, Capiati NJ. Polyethylene-polystyrene grafting reaction: effects of polyethylene molecular weight. *Polymer*. 2002; 43:4851–4858.
40. Diaz MF, Barbosa SE, Capiati NJ. Polypropylene/polystyrene blends: in situ compatibilization by Friedel-Crafts alkylation reaction. *J Polym Sci Part B: Polym Phys*. 2004;42:452–462.
41. Guo ZH, Tong LF, Fang ZP. In situ compatibilization of polystyrene/polyolefin elastomer blends by the Friedel-Crafts alkylation reaction. *Polym Int*. 2005;54:1647–1652.
42. Guo ZH, Tong LF, Xu ZB, Fang ZP. Document structure and properties of in situ compatibilized polystyrene/polyolefin elastomer blends. *Polym Eng Sci*. 2007;47:951–959.
43. Zhou W, Yu W, Zhou CX. Effect of phase morphology on the reactive blending. *Acta Polym Sin*. 2010;6:747–752.
44. Yu W, Zhou W, Zhou CX. Linear viscoelasticity of polymer blends with co-continuous morphology. *Polymer*. 2010;51:2091–2098.
45. Ha JW, Yoon Y, Leal LG. The effect of compatibilizer on the coalescence of two drops in flow. *Phys Fluids*. 2003;15:849–867.
46. Liu CY, Zhou CX, Yu W. Transesterification between poly(lactic acid) and polycarbonate under flow field and its influence on morphology of the blends. *Acta Polym Sin*. 2012;11:1225–1233.
47. Willemse RC. Co-continuous morphologies in polymer blends: stability. *Polymer*. 1999;40:2175–2178.
48. Veenstra H, van Dam J, de Boer AP. On the coarsening of co-continuous morphologies in polymer blends: effect of interfacial tension, viscosity and physical cross-links. *Polymer*. 2000;41:3037–3045.
49. Tol RT, Groeninckx G, Vinckier I, Moldenaers P, Mewis J. Phase morphology and stability of co-continuous (PPE/PS)/PA6 and PS/PA6 blends: effect of rheology and reactive compatibilization. *Polymer*. 2004;45:2587–2601.
50. Lifshitz IM, Slyozov VV. The kinetics of precipitation from supersaturated solid solutions. *J Phys Chem Solids*. 1961;19:35–50.
51. Wagner CZ. Theory of the aging of precipitates by dissolution-reprecipitation (Ostwald ripening). *Z Elektrochem*. 1961;65:581–591.
52. Binder K, Stauffer D. Theory for the slowing down of the relaxation and spinodal decomposition of binary mixtures. *Phys Rev Lett*. 1974; 33:1006–1009.
53. Siggia ED. Late stages of spinodal decomposition in binary mixtures. *Phys Rev A*. 1979;20:595–605.
54. Fortelný I, Živný A. Coalescence in molten quiescent polymer blends. *Polymer*. 1995;36:4113–4118.
55. Fortelný I, Živný A. Film drainage between droplets during their coalescence in quiescent polymer blends. *Polymer*. 1998;39:2669–2675.
56. Fortelný I, Živný A, Juza J. Coarsening of the phase structure in immiscible polymer blends. Coalescence or Ostwald ripening? *J Polym Sci Part B: Polym Phys*. 1999;37:181–187.
57. Veenstra H, van Dam J, de Boer AP. Formation and stability of co-continuous blends with a poly(ether-ester) block copolymer around its order-disorder temperature. *Polymer*. 1999;40:1119–1130.
58. Vinckier I, Laun HM. Assessment of the Doi–Ohta theory for co-continuous blends under oscillatory flow. *J Rheol*. 2001;45:1373–1385.
59. Lopez-Barron CR, Macosko CW. Rheological and morphological study of cocontinuous polymer blends during coarsening. *J Rheol*. 2012;56:1315–1334.
60. Shull KR, Kellock AJ, Deline VR, MacDonald SA. Vanishing interfacial tension in an immiscible polymer blend. *J Chem Phys*. 1992; 97:2095–2104.
61. Jiao J, Kramer EJ, de Vos S, Moller M, Koning C. Morphological changes of a molten polymer/polymer interface driven by grafting. *Macromolecules*. 1999;32:6261–6269.

62. Jiao J, Kramer EJ, de Vos S, Moller M, Koning C. Polymer interface instability caused by a grafting reaction. *Polymer*. 1999;40:3585–3588.
63. Kim JK, Jeong WY, Son JM, Jeon HK. Interfacial tension measurement of a reactive polymer blend by the Neumann triangle method. *Macromolecules*. 2000;33:9161–9165.
64. Khanna V, Kim BJ, Hexemer A, Mates TE, Kramer EJ, Li X, Wang J, Hahn SF. Chain architecture effects on the diffusion of cylinder-forming block copolymers. *Macromolecules*. 2007;40:2443–2452.
65. Fowler JN, Saito T, Gao R, Fried ES, Long TE, Green DL. Impact of diblock copolymers on droplet coalescence, emulsification, and aggregation in immiscible homopolymer blends. *Langmuir*. 2012;28:2347–2356.
66. Adedeji A, Lyu S, Macosko CW. Block copolymers in homopolymer blends: interface vs micelles. *Macromolecules*. 2001;34:8663–8668.
67. Zhang CL, Feng LF, Hoppe S, Hu GH. Instability of graft copolymers under polymer blending conditions. *Chem Eng Sci*. 2011;66:1010–1013.
68. Chambon F, Petrovic ZS, MacKnight WJ, Winter HH. Rheology of model polyurethanes at the gel point. *Macromolecules*. 1986;19:2146–2149.
69. Oshinski AJ, Keskkula H, Paul DR. The effect of polyamide end-group configuration on morphology and toughness of blends with maleated elastomers. *J Appl Polym Sci*. 1996;61:623–640.
70. DeLeo CL, Velankar S. Morphology and rheology of compatibilized polymer blends: Diblock compatibilizers vs crosslinked reactive compatibilizers. *J Rheol*. 2008;52:1385–1404.
71. Liu CY, Lin SS, Zhou CX, Yu W. Influence of catalyst on transesterification between poly(lactic acid) and polycarbonate under flow field. *Polymer*. 2013;54:310–319.
72. Palierne JF. Linear rheology of viscoelastic emulsions with interfacial tension. *Rheol Acta*. 1990;29:204–214.
73. Yang K. Rheological study of metallocene-catalyzed poly(ethylene-octene). Master thesis. Shanghai Jiao Tong University, Shanghai, 2007.
74. Riemann RE, Cantow HJ, Friedrich C. Interpretation of a new interface-governed relaxation process in compatibilized polymer blends. *Macromolecules*. 1997;30:5476–5484.
75. Jacobs U, Fahrländer M, Winterhalter J, Friedrich C. Analysis of Palierne's emulsion model in the case of viscoelastic interfacial properties. *J Rheol*. 1999;43:1495–1509.
76. van Hemelrijck E, van Puyvelde P, Velankar S, Macosko CW, Moldenaers P. Interfacial elasticity and coalescence suppression in compatibilized polymer blends. *J Rheol*. 2004;48:143–158.
77. van Hemelrijck E, van Puyvelde P, Macosko CW, Moldenaers P. The effect of block copolymer architecture on the coalescence and interfacial elasticity in compatibilized polymer blends. *J Rheol*. 2005;49:783–798.
78. Yu W, Bousmina M, Grmela M, Palierne JF, Zhou CX. Quantitative relationship between rheology and morphology in emulsions. *J Rheol*. 2002;46:1381–1399.
79. Yu W, Bousmina M, Grmela M, Zhou CX. Modeling of oscillatory shear flow of emulsions under small and large deformation fields. *J Rheol*. 2002;46:1401–1418.
80. Yu W, Zhou CX. Dynamics of droplet with viscoelastic interface. *Soft Matter*. 2011;7:6337–6346.
81. Maffettone PL, Minale M. Equation of change for ellipsoidal drops in viscous flow. *J Non-Newtonian Fluid Mech*. 1998;78:227–241.
82. Goveas JL, Fredrickson GH. Apparent slip at a polymer-polymer interface. *Eur Phys J B*. 1998;2:79–92.
83. Chang K, Morse DC. Diblock copolymer surfactants in immiscible homopolymer blends: swollen micelles and interfacial tension. *Macromolecules*. 2006;39:7746–7756.
84. Retsos H, Margiolaki I, Messaritaki A, Anastasiadis SH. Interfacial tension in binary polymer blends in the presence of block copolymers: effects of additive MW. *Macromolecules*. 2001;34:5295–5305.
85. Hu GH, Li H, Feng LF. A theoretical model for quiescent coarsening in immiscible polymer blends. *AIChE J*. 2002;48:2620–2628.
86. Torquato S, Lu B, Rubinstein J. Nearest-neighbor distribution functions in many-body systems. *Phys Rev A*. 1990;41:2059–2075.
87. Lu B, Torquato S. Nearest-surface distribution functions for polydispersed particle systems. *Phys Rev A*. 1992;45:5530–5544.
88. Lu B, Torquato S. Chord-length and free-path distribution functions for many-body systems. *J Chem Phys*. 1993;98:6472–6482.
89. McMaster LP. Aspects of liquid-liquid phase transition phenomena in multicomponent polymeric systems. *Adv Chem Ser*. 1975;142:43–65.
90. Yuan ZH, Favis BD. Coarsening of immiscible co-continuous blends during quiescent annealing. *AIChE J*. 2005;51:271–280.
91. Scholten E, Sagis LMC, van der Linden E. Coarsening rates of bicontinuous structures in polymer mixtures. *Macromolecules*. 2005;38:3515–3518.

Manuscript received Mar. 7, 2014, and revision received Sep. 10, 2014.